ACS OMEGA

Open Access

http://pubs.acs.org/journal/acsodf

Article

High Tensile, Antibacterial, and Conductive Hydrogel Sensor with Multiple Cross-Linked Networks Based on PVA/Sodium Alginate/Zinc Oxide

Yafei Qin,* Erjiong Wei, Chenkai Cui, and Jiegao Xie

Cite This: *ACS Omega* 2024, 9, 16851−16859

Read Online

ACCESS | Metrics & More | Article Recommendations | Supporting Information

ABSTRACT: Hydrogel sensors have attracted a lot of attention due to their great significance for biosensors and human detection, especially their antibacterial properties when in direct contact with the human body. However, it is challenging to improve mechanical and antibacterial performance simultaneously. In this study, by using ultrasonic dispersion technology to attach zinc oxide to cellulose and adding sodium alginate, a multiple cross-linking network is generated, which effectively solves this problem. The proposed poly(vinyl alcohol)/sodium alginate/zinc oxide/hydrogel sensor exhibits not only excellent biocompatibility but also high tensile properties (strain above 2000%). Besides, the sensor also has an antibacterial function (against *Escherichia coli* and *Staphylococcus aureus*). The hydrogel acts as a strain sensor and biosensor; it can also be used as a human health detection sensor; its high tensile properties can detect large tensile deformation and small changes in force, such as finger bending, knee bending, and other joint movements, and can also be used as a sound detection sensor to detect speech and breathing. This study provides a simple method to prepare hydrogel sensors that can be useful for human health detection and biosensor development.

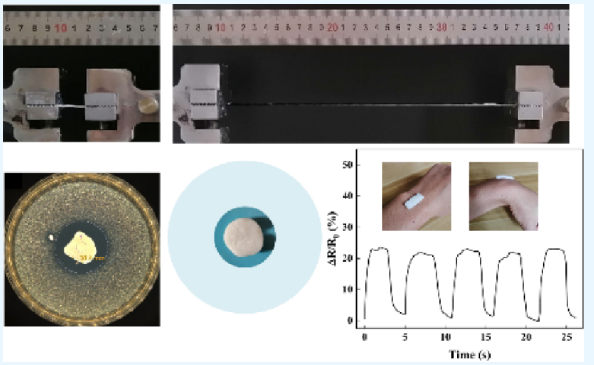

1. INTRODUCTION

Hydrogel is a flexible material with a three-dimensional (3D) network structure, formed from natural and artificial materials using various methods.[1−3] PVA (poly(vinyl alcohol)) and sodium alginate are commonly used hydrogels due to their favorable physical and chemical properties, finding applications in diverse fields such as biomedicine,[4−6] wearable devices,[7−9] drug delivery,[10] electronic skin,[11−14] and sensors.[15−17] Presently, there is a demand for sensors in human health detection that possess wide applicability, ultrahigh stretchability, and exhibit good antibacterial activity against both Gram-positive and Gram-negative bacteria. To satisfy the desired performance, it is necessary to synthesize critical materials. Adding ZnO was an effective strategy for developing hydrogel-based sensors with antibacterial capabilities for human health monitoring. Zinc plays an essential role in biological antibacterial processes because of its effect primarily stem from zinc ion release and membrane dysfunction.[18−21]

Hydrogels have attracted a lot of attention from industry and the medical community due to their excellent properties. For hydrogels, there are two types of cross-links, both physical and chemical cross-linking. Many researchers also use multiple cross-linking methods.[22,23] Among them, Ramzan et al.[24] utilizing the freeze gelation technique developed chitosan-sodium alginate-elastin-based nanocomposite scaffolds with ZnO-NPs that provided a moist environment while exhibiting antimicrobial activity. These scaffolds demonstrated excellent mechanical strength, cost-effectiveness, and antibacterial properties alongside high wound exudate absorption capacity; they were also degradable under room temperature conditions, offering stability benefits. Cross-linking of multiple networks often results in hydrogels with high tensile properties, but causes other performance degradation comparatively. After years of development, with the efforts of numerous researchers, hydrogels have various properties, such as antibacterial properties,[25,26] self-healing properties,[27,28] strain sensing properties,[29] expansion and contraction properties,[30] and EMI application properties.[31] It is an important research direction to combine these properties in multiple networks. Gao et al.[32] obtained wound dressings with high adhesion, biocompatibility, the ability to promote tissue regeneration through a simple one-pot synthesis, and can be dried into disposable patches that are conducive to long-term storage and field use. Zeng et al.[33] constructed a physically cross-linked PVA/CS-PA conductive hydrogel with recyclable, healing, and

Received: February 26, 2024
Revised: March 5, 2024
Accepted: March 15, 2024
Published: March 26, 2024

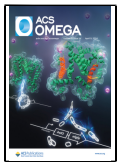

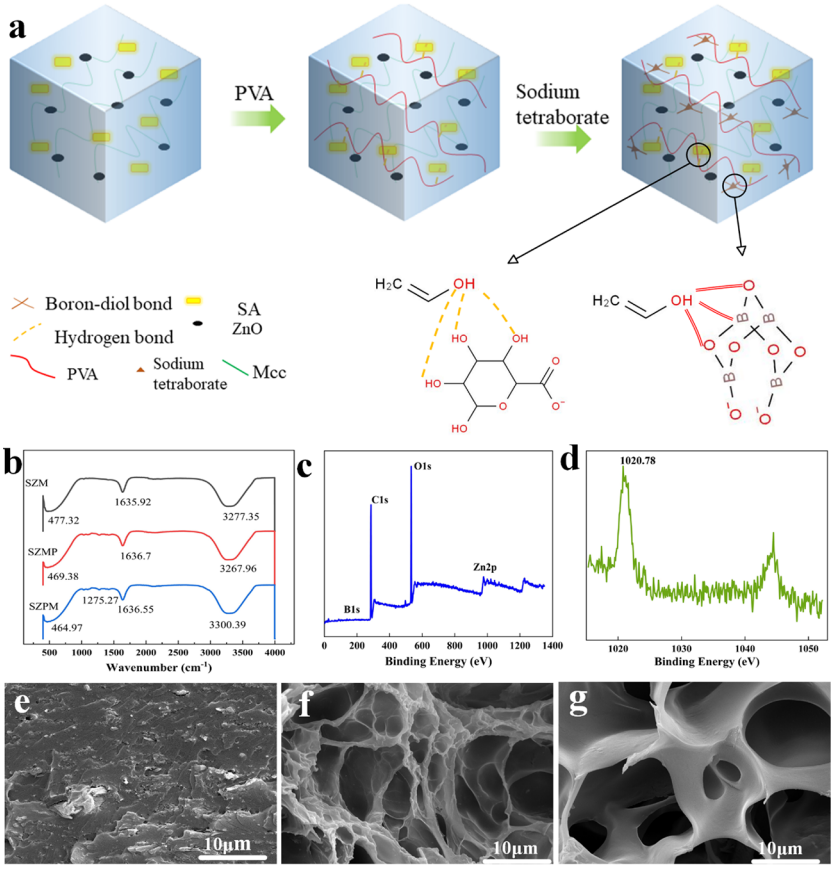

Figure 1. (a) SZPM hydrogel preparation diagram includes the possible hydrogen bonding of PVA with sodium alginate and the dynamic boron-diol bonding of PVA with borax. (b) FTIR map of SZM, SZMP, and SZPM hydrogel. (c) XPS full spectrum scan of SZPM hydrogel. (d) Zn 2p fine spectrum of SZPM hydrogel. 10 μm SEM images of (e) ZPM hydrogel, (f) S_1ZPM hydrogel, and (g) S_2ZPM hydrogel.

antibacterial properties through a simple freeze−thaw method. It exhibits mechanical flexibility (~200 kPa stress, ~ 650% elongation) and self-recovery ability and has antibacterial activity against Gram-positive and Gram-negative bacteria. Hydrogels are key to drug delivery because of their biocompatibility,[34] etc. However, there are few studies on the antibacterial properties and wound dressing of hydrogels as stretchable patch sensors, and further studies are needed for the future application of hydrogels.

The hydrogel made in this study is based on PVA, sodium alginate, and microcrystalline cellulose, adding zinc oxide, and using ultrasonic dispersion technology to make it adhere to microcrystalline cellulose so that the hydrogel has antibacterial properties. Then mix in borax was mixed to create two cross-linked networks that generate dynamic boron-diol bonds (PVA chain cross-linked with borax) and hydrogen bonds (PVA cross-linked with sodium alginate). The added cellulose forms a new conductive network, which makes the hydrogel reach a three-layer cross-linking network. Therefore, hydrogels have excellent tensile properties and good antibacterial properties and maintain long-term reliability. The electromechanical property test shows that the tensile strain reaches more than 2000%, the tensile strength reaches 18.42 kpa, and the GF value is higher than 3.45. As a wound filler, the SZPM (sodium alginate/zinc oxide/poly(vinyl alcohol)/microcrystalline cellulose) hydrogel can be placed on the wound continuously to avoid the possibility of cross-infection caused by multiple dressing changes. Moreover, it can detect the movement of various parts of the body, such as fingers, wrists, neck, and knees, and it can also detect different sounds and respond to them. This method has great application value for future human health detection sensors.

2. MATERIALS AND PREPARATORY PROCEDURES APPLIED

2.1. Preparatory Procedures Applied. PVA 235 (alcoholysis degree 87−89%(mol/mol)) was obtained from Shanghai Macklin Biochemical Technology Co., Ltd. Sodium alginate (SA) was obtained from Sinopharm Chemical Reagent Co., Ltd. Microcrystalline Cellulose (MCC particle size −20−100 μm) was obtained from Sinopharm Chemical Reagent Co., Ltd. Zinc oxide was obtained from Qing he County Xinhu Metal Material Co., Ltd. Sodium tetraborate decahydrate was obtained from Shanghai Macklin Biochemical Technology Co., Ltd. All chemical reagents were used directly without any further treatment.

2.2. Equipment Setup. A universal testing machine (ZQ-950B, zhiqu Instruments, Dongguan, China) was used to characterize the mechanical properties of the hydrogel. The strain sample size was 30 × 10 × 3 mm^3, and the experimental loading rate was 100 mm/min. The compressed sample size was 12 mm in diameter, 12 mm in height, and the test speed was 30 mm/min. LCR measurement instrument (TH2830, TongHui, China) was used to detect the resistance of the hydrogel in the motion of human joints. The microstructure of the hydrogel was analyzed by scanning electron microscopy (SEM Thermo Fisher Quattro S). The elemental composition of the hydrogel was detected by X-ray photoelectron

https://doi.org/10.1021/acsomega.4c01860
ACS Omega 2024, 9, 16851−16859

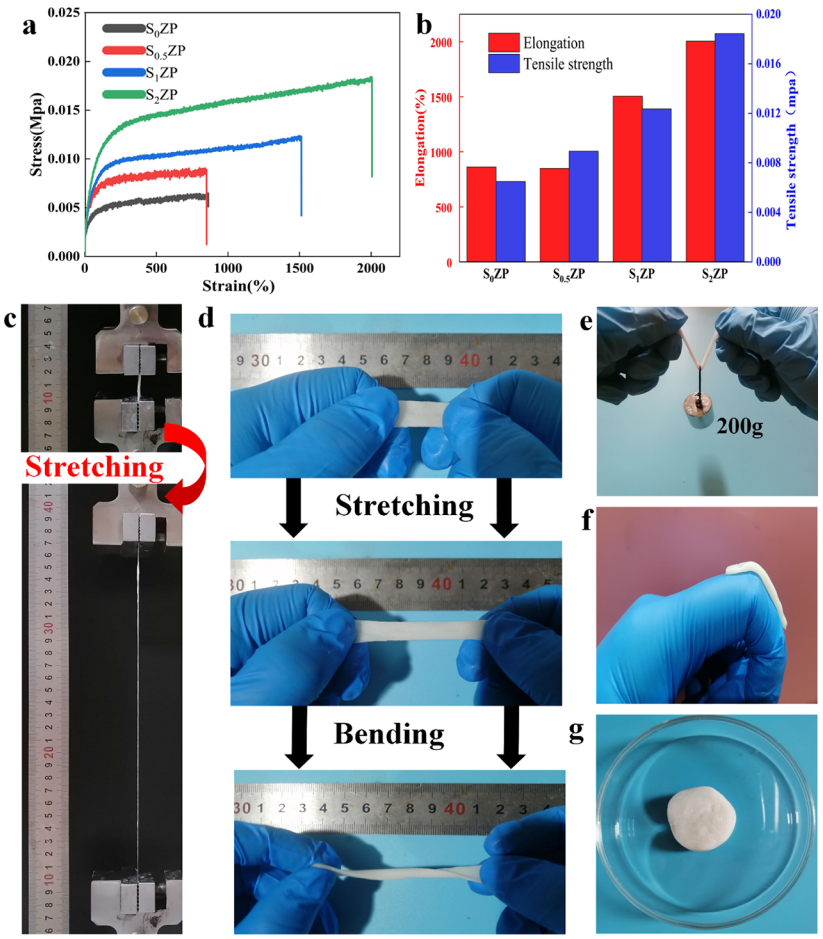

Figure 2. Mechanical properties of hydrogel: (a) stress−strain curves of different 0%, 0.5%, 1%, and 2% SA contents. (b) Elongation at break (red) and tensile strength (blue). (c) Shape dimensions of hydrogels before stretching and shape dimensions of hydrogels after stretching. (d) Hydrogel stretching and twisting. (e) Lifting a weight. (f) Finger bending. (g) Physical drawing of the hydrogel.

spectroscopy (XPS Thermo Fisher Nex). The conformational structure and chemical composition of the prepared nanocomposite scaffolds were analyzed using Fourier transform infrared spectrometer detection (FTIR Thermo Nicolet iS5) in the spectral range of 400 cm^{-1} to 4000 cm^{-1}.

2.3. Antimicrobial Testing and Biocompatibility Test. The antibacterial properties of the hydrogel were investigated. First, the hydrogel was treated with UV irradiation for 2 h, and then the test bacteria were cultured until obvious plaque was observed. After the bacteria-containing medium was solidified, it was put into the test hydrogel and incubated at 37 °C for 24 h. The size of the bacterial inhibition zone was photographed and analyzed to observe the inhibition zone around each sample. The biocompatibility of the hydrogel was studied by the MTT method. First, the sample was irradiated by ultraviolet light for 30 min, and HeLa cells were placed in the hydrogel solution with different concentrations for 48 h. Then, cell activity was observed by laser confocal fiber imaging.

2.4. Hydrogel Preparation. We added 0.3 g of sodium alginate to 29.7 g of water and stirred evenly at low speed, and 0.1 g of zinc oxide was added into it and stirred for 6 h. The sample was sonicated at 300 W for half an hour and then stirred for 1 h. After adding 0.3 g of MCC, stirred overnight, and then sonicated at 300 W for half an hour, then added 8% content of PVA and stirred until uniform, and then added quantitative borax solution and formed. The preparation process is shown in Figure 1a.

3. RESULTS AND DISCUSSION

3.1. Hydrogel Characterization. The preparation process of the SZPM hydrogel is shown in Figure 1a. In this preparation process, with the continuous addition of materials, first, a hydrogen bond connection was generated between PVA and sodium alginate, and then the added sodium tetraborate also combined with PVA to produce dynamic boron-diol bonds, resulting in two kinds of cross-linking networks inside the hydrogel. The hydrogel underwent a chemical analysis. Figure 1b presents the FTIR analysis spectrum of S_2ZPM hydrogel, revealing prominent peaks at 464.97 cm^{-1},1275.27 cm^{-1}, 1636.55 cm^{-1}, and 3300.39 cm^{-1}. Compared with other FTIR diagrams, the FTIR of SZPM showed a peak at 1275.27 cm^{-1} indicating B−O−C bending vibration, suggesting the formation of dynamic boron-diol bonds between PVA and sodium tetraborate in the hydrogel.[35] The broad peak observed at 3300.39 cm^{-1} signifies O−H stretching vibration resulting from hydrogen bonding between PVA and sodium alginate.[36] Additionally, a C═C skeleton vibration is recorded at 1636.55 cm^{-1}. Thus, two bonding modes are present in the hydrogel: hydrogen bonding between PVA and sodium alginate as well as a dynamic boron-diol bonding network. In addition, in the case of cellulose-zinc oxide-sodium alginate nanocomposite fiber,

https://doi.org/10.1021/acsomega.4c01860
ACS Omega 2024, 9, 16851−16859

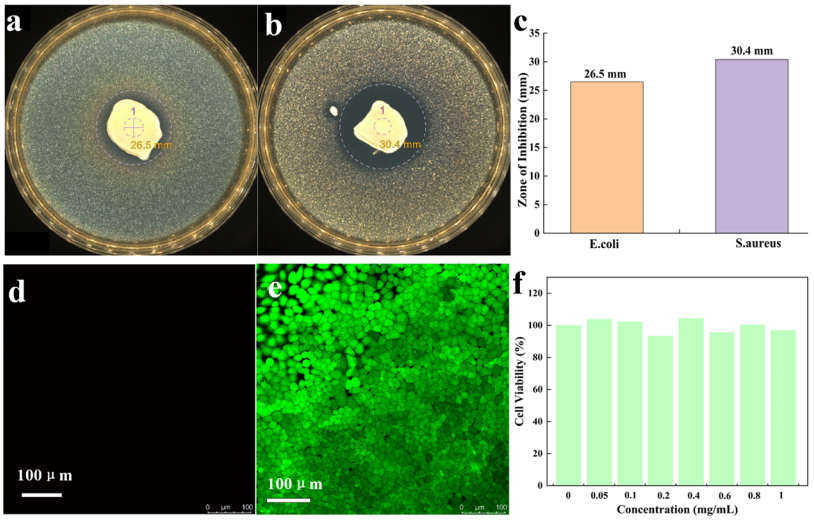

Figure 3. Antibacterial properties and biocompatibility of hydrogels. Schematic diagram of the antibacterial effect of S_2ZPM hydrogel against (a) *E. coli*, (b) *S. aureus*, and (c) S_2ZPM hydrogel against *E. coli* and *S. aureus* antibacterial bar diagram. (d) Dead (red fluorescence) and (e) living (green fluorescence) CLSM images of HeLa cells cultured in a 1 mg/mL extract solution of SZPM. (f) Biocompatibility test.

the peak value of Zn−O−Zn vibration was found at 464.97 cm^{-1}, which is different from the common ZnO peak value, indicating the composite bonding property of nanozno with microcrystalline cellulose under a sodium alginate matrix.[37] Figure 1c displays an XPS full-spectrum scan confirming the presence of elements, such as B 1s, C 1s, O 1s, and Zn 2p. Two distinct high peaks are noticeable in this figure: one corresponding to carbon (C) at an energy level of approximately 286.08 eV and another representing oxygen (O) at around 533.08 eV. Furthermore, a few weak but notable peaks can be observed in the XPS scan of the hydrogel including a zinc (Zn) peak at 1020.78 eV. Figure 1d depicts a specific fine scan, revealing the obvious characteristic peaks associated with zinc in the hydrogel. The characteristic peaks of B 1s and C 1s are shown in Figure s1. Figure 1e−g shows a 10 μm SEM image of the ZPM hydrogel, S_1ZPM hydrogel, and S_2ZPM hydrogel. On the SEM image of 10 μm, the void of hydrogel increased with the increase in sodium alginate content, and the conductivity increased. It is clear that the hydrogel presents a 3D structure with an abundance of condensation. It can be seen that after simple treatment, each hydrogel material has been cross-linked by the hydrogen bond between SA and PVA and the complexation reaction between borax, and no significant nonbonded material can be seen on the SEM image.[38]

3.2. Mechanical Property Test. To investigate the impact of different SA contents on the mechanical strength and toughness of the SZPM hydrogel, a tensile test was conducted. This is shown in Figure 2a,b. The results showed that the mechanical properties of the hydrogel with 2% SA were significantly improved compared to those without SA. As the mass of SA increased from 0%, 0.5%, 1%, to 2%, the tensile stresses and strains also increased accordingly, the tensile stresses of the hydrogel were 6.48 8.93, 12.35, and 18.42 KPa, respectively, and the tensile strains were 862%, 848%, 1505%, and 2006%, indicating a positive correlation between SA content and mechanical property enhancement. However, physical cross-linked hydrogen bond bonding between PVA and sodium tetraborate in the hydrogel did not improve its mechanical properties without SA addition, resulting in lower values for both tensile stress and strain than those with added SA. Nevertheless, a small amount of SA could not sufficiently react with PVA to form a hydrogen bond connection, leading to little change in tensile strain when comparing samples containing 0% or 0.5% of SA. With further increase in SA content, however, significant improvement was observed in terms of both tensile stress and strain performance; specifically speaking, SZPM hydrogel at an optimal concentration level (i.e., 2%), this improvement reached as high as 2.3 times for strain value while nearly 3-fold for stress value compared to without SA hydrogel. Figure 3c shows a drawing diagram of hydrogel stretching. As the stretching rate increases, the hydrogen bond network connected inside the hydrogel breaks to a certain extent, until the hydrogel breaks into two pieces, and the dynamic boron-diol bond is completely broken. When the hydrogel with different SA contents was broken, the stress−strain curve of the hydrogel did not have a certain bend and then linearly decreased, but directly broke when it reached the limit value of strain. The addition of SA not only affects the tensile properties but also provides excellent electrical conductivity for the hydrogel.[39] The addition of excessive SA leads to poor strain performance of the hydrogel, so the following study focuses on the performance of the S_2ZPM hydrogel.

Mechanical properties are among the most important properties of flexible sensors. As shown in Figure 2c, hydrogels have ultrahigh tensile properties, which are highly feasible for applications requiring high tensile properties. Hydrogels have brittleness caused by zinc oxide addition while also affecting their transparency.[40] Figure 2d shows that the hydrogel can have good torsion after stretching, indicating the versatility of the hydrogel in complex situations. Figure 2e shows that its hydrogel can lift a weight of 200 g, indicating that the hydrogel has excellent mechanical strength. At the same time, the hydrogel also has good bending and shaping capability, as shown in Figure 2f,g.

3.3. Biocompatibility and Antimicrobial Properties. In life, it is inevitable that injuries result in abrasions and broken skin wounds, particularly affecting vulnerable joint parts like the elbow joint. Such injuries cause bruising and bleeding on the surface of the human body, leading to inflammation. The presence of external bacteria can enter through these wounds,

https://doi.org/10.1021/acsomega.4c01860
ACS Omega 2024, 9, 16851−16859

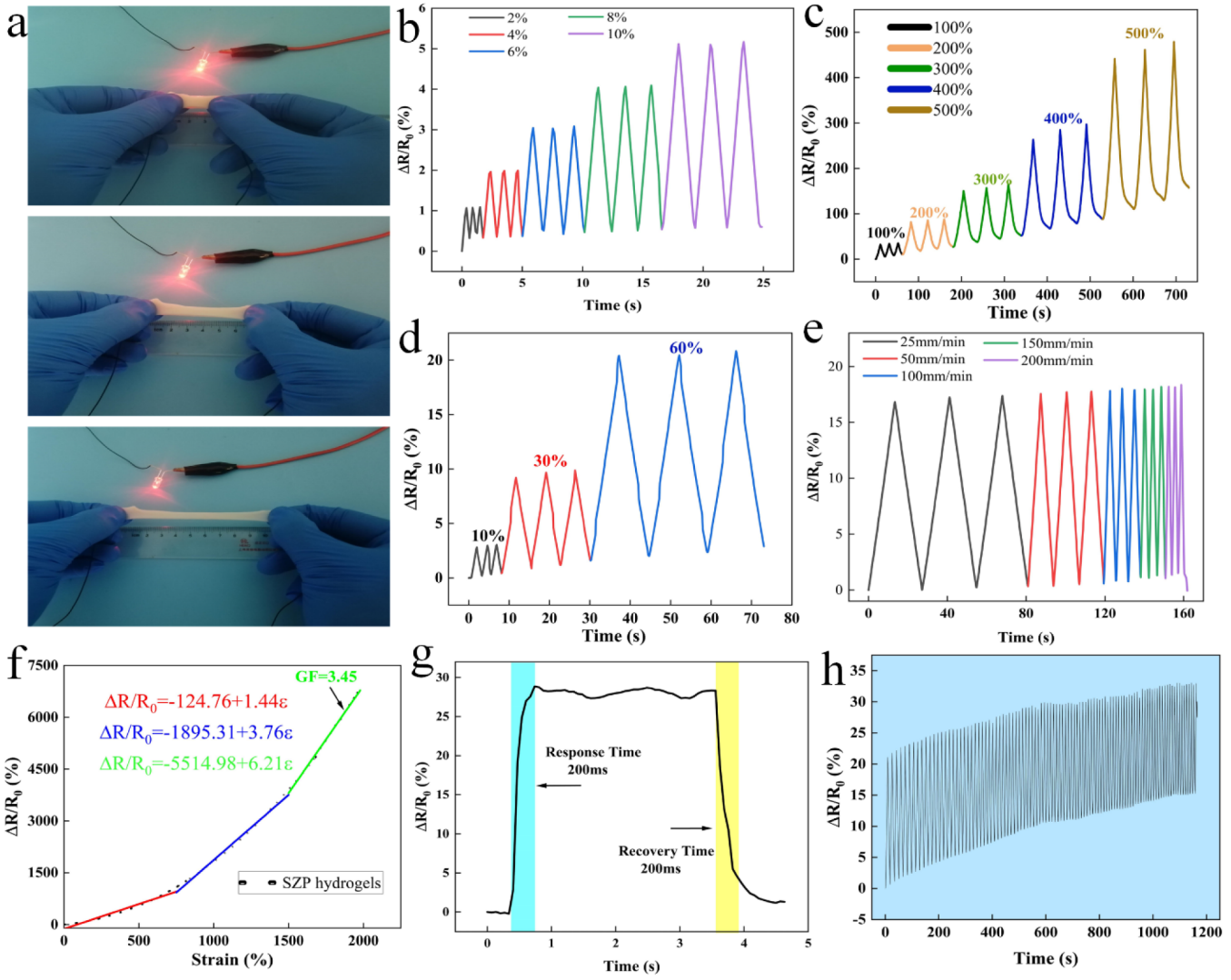

Figure 4. Electrical properties of hydrogels. (a) As the hydrogel strain increases, the brightness of the bulb decreases. (b) The relative resistance of hydrogel at low strain of 2%, 4%, 6%, 8%, and 10%. (c) Relative resistance changes of SZPM hydrogel at the speed of 100 mm/min at 100%, 200%, 300%, 400%, and 500% under strain. (d) Relative resistance changes of S_2ZPM hydrogel at the speed of 100 mm/min at 10%, 30%, and 60% under low strain. (e) Change of relative resistance under the same strain of 25 mm/min, 50 mm/min, 100 mm/min, 150 mm/min, and 200 mm/min at different speeds. (f) The relationship between S_2ZPM hydrogel strain and its relative resistance. (g) Response time of the sensor under rapid stretching and recovery. (h) The relative resistance change of SZPM hydrogel under 50% strain for 100 cycles.

potentially impacting wound healing. The sensor with antibacterial performance developed in this paper can be precisely used in these scenarios. To demonstrate the antibacterial properties, we tested its activity against *Staphylococcus aureus* and *Escherichia coli*strains using the disk diffusion method. Zinc oxide exhibits excellent antibacterial effects without adverse effects on the human body; moreover, the trace element zinc has a positive effect on wound healing.[41] Over time, zinc ions released from the hydrogel damaged both *S. aureus* and *E. coli* in Petri dishes, resulting in color changes near the hydrogel as well as within the original Petri dish medium. The hydrogel exhibited an antibacterial ring size of 26.5 mm for *E. coli* and 30.4 mm for *S. aureus* as shown in Figure 3c. The extent of the color change surrounding the hydrogel indicates its level of antibacterial activity. These results highlight that our hydrogel possesses significant antibacterial activity against both *S. aureus* and *E. coli* strains, consistent with findings reported by other researchers.[42−44] The biological activity of HeLa cells cultured with 1.0 mg/mL of SZPM hydrogel extract was directly determined by a confocal laser scanning microscope (CLSM). There was basically no red light in the dead light photograph in Figure 3d, while green light was evident in most areas in Figure 3e. In Figure 3f, HeLa cells were cultured with extracts of the SZPM hydrogel of different concentrations (0.05−1.0 mg/mL), and cell viability was tested. The results showed that HeLa cells had a cell survival rate of more than 90% at all tested concentrations. This indicates that SZPM hydrogels have good biocompatibility. It can be used as a new way of biosensor and wound packing in the future. As shown in Figure s3, the resistance of the SZPM hydrogel changes greatly with the reduction of mass.

3.4. Electrical Performance. The sensing performance of the hydrogel sensor was investigated to demonstrate its stable applicability in human health detection. The detection both of large strains and small strains has always been an important challenge for hydrogel sensors.[45] The SZPM hydrogel sensor developed in this study accomplished the detection of small

https://doi.org/10.1021/acsomega.4c01860
ACS Omega 2024, 9, 16851−16859

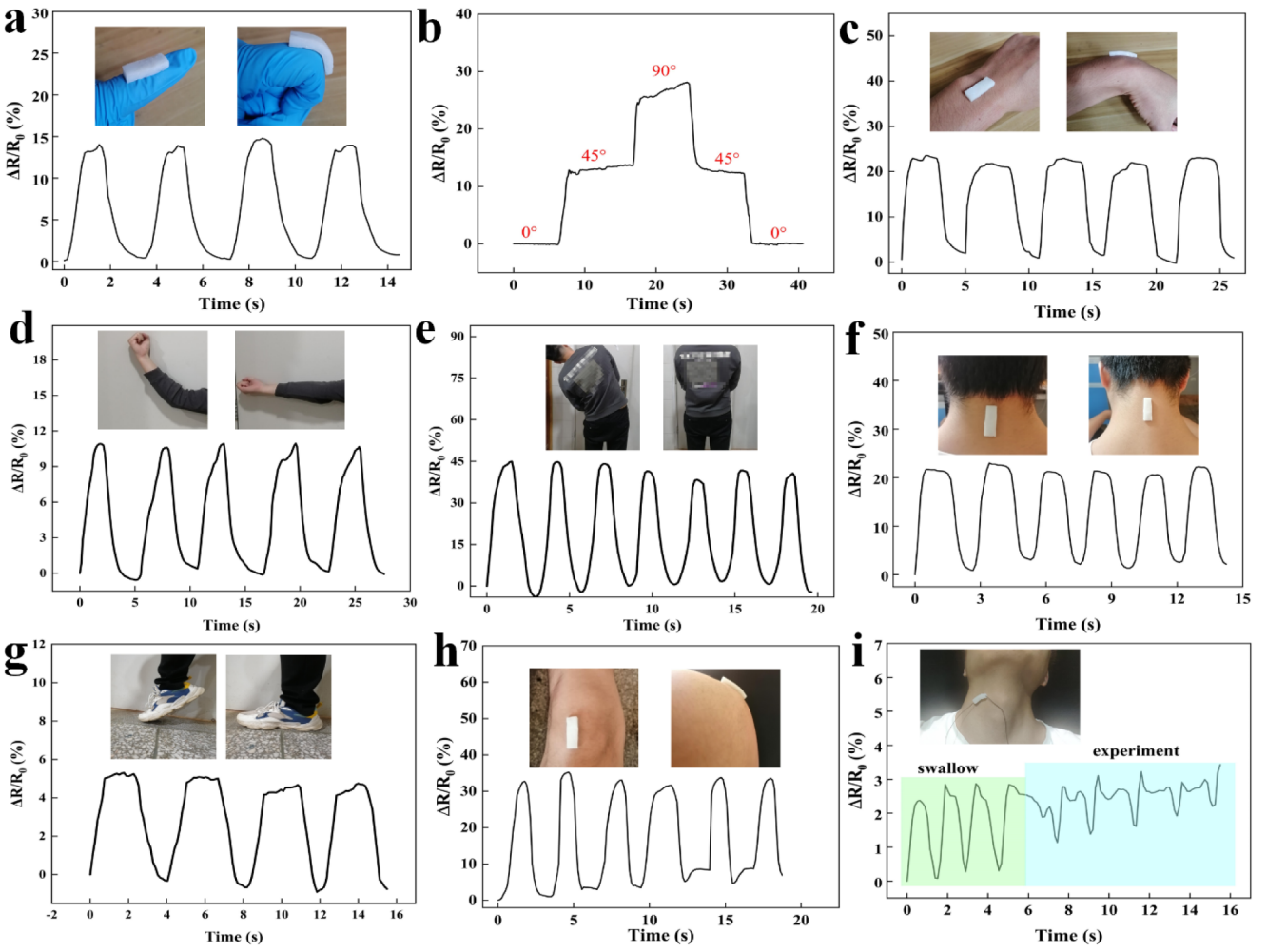

Figure 5. Hydrogel for human motion detection. Human movement was detected using SZPM hydrogel sensors: (a) fingers, (b) fingers bent at different angles, (c) wrist, (d) elbow, (e) waist twisting, (f) neck bending, (g) ankle, (h) knee bending, and (i) throat swallowing and speaking.

and large strain ranges through the physical and chemical cross-linking generated between PVA and SA and borax. SZPM hydrogels contain a variety of ions. When the hydrogel is connected to the power supply, the ions theoretically move from the positive electrode to the negative electrode, thus making the hydrogel conductive. For hydrogels with different contents of sodium alginate, the conductivity of the hydrogels is not different, and the conductivity of the hydrogels increases with the increase of sodium alginate content, as shown in Figure s2. Hydrogels with sodium alginate added are significantly more conductive than those without, because sodium alginate, as an electrolyte, is ionized in water to release a large number of free ions, thereby improving conductivity.[46] As the tensile strain gradually increases, the brightness of the bulb also darkens, as shown in Figure 4a. As depicted in Figure 4b−d the relative resistance of the hydrogel exhibits noticeable changes under small, medium, and large strains, while it remains relatively stable within the same strain range, indicating excellent resistance stability of the sensor. That is, the relative resistance of the hydrogel can still have a significant difference in the strain difference of 2%. Additionally, the relative resistance also demonstrates high stability under large strains with gradual increase along with increasing strain magnitude, revealing a strong correlation between hydrogel resistance and strain level. Another proof of the stability of hydrogels is that the relative resistance changes of hydrogels under the same strain and different speeds are slightly different, as shown in Figure 4e. GF is an essential indicator for sensor sensitivity represented by the formula $GF = \Delta R/R_0/\varepsilon$. As illustrated in Figure 4f, it is divided into three segments: 0−750% $\Delta R/R_0 = -124.76 + 1.44\varepsilon$, 750%−1500% $\Delta R/R_0 = -1895.31 + 3.76\varepsilon$, and 1500%−2000% $\Delta R/R_0 = -5514.98 + 6.21\varepsilon$; the maximum GF value reaches up to 3.45 which is significantly higher than other types of hydrogels.[47,48] Figure 4g shows the response time of the sensor under rapid stretching and recovery. Furthermore, Figure 4h indicates that our sensor can stably output relative resistance change even after undergoing repetitive testing involving up to one hundred times at 50% strain level, suggesting reliable, sturdy, and durable characteristics suitable for use as sensors for human sports health detection. In Figure s4, it is shown that hydrogels have the performance of pressure detection. Hydrogels can clearly distinguish different pressures and can carry out more than 100 pressure cycles while maintaining a certain stability. In Table s1, the main performance parameters of this paper are compared with those of previous papers. It can be seen from the table that although the parameters of this paper have some shortcomings compared with those of previous papers, overall, the comprehensive performance of this paper is better than that of previous papers.

https://doi.org/10.1021/acsomega.4c01860
ACS Omega 2024, 9, 16851−16859

3.5. Sensing Performance. For sensors, detecting body motion data is where flexible sensors outperform other sensors. The wrist and fingers of the human body are an integral part of regular movement, and the increasing number of sedentary people, in particular, has led to more finger movements; therefore, sensors to detect fingers and wrists have become increasingly available. Figure 5a shows that the relative resistance changes detected by the hydrogel sensor during the back-and-forth up-and-down motion of the finger are well stabilized. A more accurate detection is that the relative change in resistance also changes when the finger is bent at different angles, as shown in Figure 5b. The relative change in resistance of the finger is the same at 0°, 45°, and 90°. Figure 5c–h is about the detection of human wrist, neck, and knee joint and other different joint movements. It can be seen the resistance change of the sensor varies with different detection positions, showing that the hydrogel can detect various body parts of the human body, indicating the wide detecting application is a relatively important ability of flexible sensors, which are used to fit the human body for sensing signal output.[49] In addition to body motion detection, the SZPM hydrogel can also detect throat sounds and swallowing. Figure 5i shows that the relative resistance changes are relatively stable and have a high degree of similarity during throat swallowing. When "experiment" is completed, the relative change rule of resistance is even the same. As can be seen from the above, the SZPM hydrogel sensor provides a novel approach to human body detection. Not only were the movements of the various joints of the human body detected but also the differences in the sound of the voice and the swallowing of the throat.

4. CONCLUSION

In summary, this paper has developed a hydrogel sensor with ultrahigh stretching, antibacterial properties, and visual ability of wound healing. PVA and sodium alginate are the main materials to generate multiple cross-linked networks, which have good biocompatibility and can be perfectly applied to human skin. Moreover, the sensor preparation process is simple and reproducible. Microscopic images of the hydrogel show that after two ultrasonic treatments, zinc oxide has been deeply embedded in the cellulose, and the cellulose is also embedded in the structure of the hydrogel, forming a good three-dimensional structure. With the gradual increase of sodium alginate, the dynamic boron-diol bonding and hydrogen bonding of the hydrogel improve the mechanical properties of the hydrogel. The tensile strength of SZPM hydrogel reaches 18.42 kpa, and the elongation at break reaches 2006%, indicating its superior tensile capacity. The addition of zinc oxide increased the antibacterial activity of the hydrogel. In vitro antibacterial tests showed that the hydrogel had good antibacterial activity against *E. coli* and *S. aureus*. In addition, hydrogels have excellent electrical properties. When used as wound fillers, hydrogels have the ability to visualize wound healing due to the change of hydrogel resistance caused by wound healing. SZPM hydrogel sensor is also capable of detecting sound vibration and joint motion. This study provides a promising avenue for future health monitoring applications.

■ ASSOCIATED CONTENT

Supporting Information

The Supporting Information is available free of charge at https://pubs.acs.org/doi/10.1021/acsomega.4c01860.

Figure s1: B 1s and C 1s fine spectrum of SZPM hydrogel, Figure s2: hydrogel conductivity with different sodium alginate contents, Figure s3: diagram of hydrogel resistance variation in wound healing response, Figure s4: compression performance of SZPM hydrogel, and Table 1 compares the key performance parameters of the hydrogels in this paper with those reported previously (PDF)

■ AUTHOR INFORMATION

Corresponding Author

Yafei Qin − *Faculty of Mechanical and Electrical Engineering, Kunming University of Science and Technology, Kunming 650093, China;* orcid.org/0000-0002-6586-2774; Email: qinyafei_kmust@foxmail.com

Authors

Erjiong Wei − *Faculty of Mechanical and Electrical Engineering, Kunming University of Science and Technology, Kunming 650093, China;* orcid.org/0009-0002-7359-325X

Chenkai Cui − *Faculty of Mechanical and Electrical Engineering, Kunming University of Science and Technology, Kunming 650093, China*

Jiegao Xie − *Faculty of Mechanical and Electrical Engineering, Kunming University of Science and Technology, Kunming 650093, China*

Complete contact information is available at: https://pubs.acs.org/10.1021/acsomega.4c01860

Author Contributions

The manuscript was written through contributions of all authors. All authors have given approval to the final version of the manuscript.

Funding

This work was supported in part by the National Natural Science Foundation of China under Grant 52165066, the General Research Project of Yunnan Province under Grant 202101AT070106, and the Xingdian Talent Support Program Youth Project of Yunnan Province under Grant 2022.

Notes

The authors declare no competing financial interest.

■ REFERENCES

(1) Jiang, X.; Xiang, N.; Zhang, H.; Sun, Y.; Lin, Z.; Hou, L. Preparation and characterization of poly(vinyl alcohol)/sodium alginate hydrogel with high toughness and electric conductivity. *Carbohydr. Polym.* **2018**, *186*, 377−383.

(2) Xu, C.; Guan, S.; Dong, X.; Qi, M. Super strong gelatin/cellulose nanofiber hybrid hydrogels without covalent cross-linking for strain sensor and supercapacitor. *Composites, Part A* **2023**, *164*, 107287.

(3) Lu, X.; Zeng, Y.; Yang, Y.; Yang, X.; Wei, E.; Cui, C.; Xie, J.; Qin, Y.; Qian, Z. PVA/PA/H3PO4 Hydrogel Films with Ultrawide Pressure and Strain Sensing Range via Facile Fabrication Method. *Adv. Mater. Technol.* **2023**, *8* (13), 2202123.

(4) Ma, R.; Wang, Y.; Qi, H.; Shi, C.; Wei, G.; Xiao, L.; Huang, Z.; Liu, S.; Yu, H.; Teng, C.; Liu, H.; Murugadoss, V.; Zhang, J.; Wang, Y.; Guo, Z. Nanocomposite sponges of sodium alginate/graphene oxide/polyvinyl alcohol as potential wound dressing: In vitro and in vivo evaluation. *Composites, Part B* **2019**, *167*, 396−405.

(5) Hu, O.; Chen, G.; Gu, J.; Lu, J.; Zhang, J.; Zhang, X.; Hou, L.; Jiang, X. A facile preparation method for anti-freezing, tough, transparent, conductive and thermoplastic poly(vinyl alcohol)/

sodium alginate/glycerol organohydrogel electrolyte. *Int. J. Biol.Macromol.* **2020**, *164*, 2512−2523.
(6) Xu, J.; Tsai, Y. L.; Hsu, S. H. Design Strategies of Conductive Hydrogel for Biomedical Applications. *Molecules* **2020**, *25* (22), 5296.
(7) Liu, C.; Wang, X.; Zhang, H. J.; You, X.; Yue, O. Self-Healable High-Strength Hydrogel Electrode for Flexible Sensors and Supercapacitors. *ACS Appl. Mater. Interfaces* **2021**, *13* (30), 36240−36252.
(8) Wei, J.; Xie, J.; Zhang, P.; Zou, Z.; Ping, H.; Wang, W.; Xie, H.; Shen, J. Z.; Lei, L.; Fu, Z. Bioinspired 3D Printable, Self-Healable, and Stretchable Hydrogels with Multiple Conductivities for Skin-like Wearable Strain Sensors. *ACS Appl. Mater. Interfaces* **2021**, *13* (2), 2952−2960.
(9) Song, B.; Dai, X.; Fan, X.; Gu, H. Wearable multifunctional organohydrogel-based electronic skin for sign language recognition under complex environments. *J. Mater. Sci. Technol* **2024**, *181*, 91−103.
(10) Ren, S.; Liu, H.; Wang, X.; Bi, J.; Lu, S.; Zhu, C.; Li, H.; Kong, W.; Chen, R.; Chen, Z. Acupoint nanocomposite hydrogel for simulation of acupuncture and targeted delivery of triptolide against rheumatoid arthritis. *J. Nanobiotechnol.* **2021**, *19* (1), 409.
(11) Wang, Z.; Bu, T.; Li, Y.; Wei, D.; Tao, B.; Yin, Z.; Zhang, C.; Wu, H. Multidimensional Force Sensors Based on Triboelectric Nanogenerators for Electronic Skin. *ACS Appl. Mater. Interfaces* **2021**, *13* (47), 56320−56328.
(12) Zhang, D.; Jian, J.; Xie, Y.; Gao, S.; Ling, Z.; Lai, C.; Wang, J.; Wang, C.; Chu, F.; Dumont, M.-J. Mimicking skin cellulose hydrogels for sensor applications. *Chem. Eng. J.* **2022**, *427*, 130921.
(13) Zhang, Y.; Yang, J.; Hou, X.; Li, G.; Wang, L.; Bai, N.; Cai, M.; Zhao, L.; Wang, Y.; Zhang, J.; et al.et al. Highly stable flexible pressure sensors with a quasi-homogeneous composition and interlinked interfaces. *Nat. Commun.* **2022**, *13* (1), 1317.
(14) Fan, X.; Ke, T.; Gu, H. Multifunctional, Ultra-Tough Organohydrogel E-Skin Reinforced by Hierarchical Goatskin Fibers Skeleton for Energy Harvesting and Self-Powered Monitoring. *Adv. Funct. Mater.* **2023**, *33* (42), 2304015.
(15) Chen, D.; Zhao, X.; Wei, X.; Zhang, J.; Wang, D.; Lu, H.; Jia, P. Ultrastretchable, Tough, Antifreezing, and Conductive Cellulose Hydrogel for Wearable Strain Sensor. *ACS Appl. Mater. Interfaces* **2020**, *12* (47), 53247−53256.
(16) Lu, X.; Qin, Y.; Chen, X.; Peng, C.; Yang, Y.; Zeng, Y. An ultra-wide sensing range film strain sensor based on a branch-shaped PAN-based carbon nanofiber and carbon black synergistic conductive network for human motion detection and human−machine interfaces. *J. Mater. Chem. C* **2022**, *10* (16), 6296−6305.
(17) Li, Y.; Liu, X.; Gong, Q.; Xia, Z.; Yang, Y.; Chen, C.; Qian, C. Facile preparation of stretchable and self-healable conductive hydrogels based on sodium alginate/polypyrrole nanofibers for use in flexible supercapacitor and strain sensors. *Int. J. Biol. Macromol.* **2021**, *172*, 41−54.
(18) Qi, K.; Cheng, B.; Yu, J.; Ho, W. Review on the improvement of the photocatalytic and antibacterial activities of ZnO. *J. Alloys Compd.* **2017**, *727*, 792−820.
(19) Lallo da Silva, B.; Caetano, B. L.; Chiari-Andreo, B. G.; Pietro, R.; Chiavacci, L. A. Increased antibacterial activity of ZnO nanoparticles: Influence of size and surface modification. *Colloids Surf., B* **2019**, *177*, 440−447.
(20) Abebe, B.; Zereffa, E. A.; Tadesse, A.; Murthy, H. C. A. A Review on Enhancing the Antibacterial Activity of ZnO: Mechanisms and Microscopic Investigation. *Nanoscale Res. Lett.* **2020**, *15* (1), 190.
(21) Jiang, S.; Lin, K.; Cai, M. ZnO Nanomaterials: Current Advancements in Antibacterial Mechanisms and Applications. *Front. Chem.* **2020**, *8*, 580.
(22) Mu, G.; He, W.; He, J.; Muhammad, Y.; Shi, Z.; Zhang, B.; Zhou, L.; Zhao, Z.; Zhao, Z. High strength, anti-freezing and conductive silkworm excrement cellulose-based ionic hydrogel with physical-chemical double cross-linked for pressure sensing. *Int. J. Biol. Macromol.* **2023**, *236*, 123936.
(23) Wu, J.; Wu, X.; Yang, F.; Liu, X.; Meng, F.; Ma, Q.; Che, Y. Multiply cross-linked poly(vinyl alcohol)/cellulose nanofiber composite ionic conductive hydrogels for strain sensors. *Int. J. Biol. Macromol.* **2023**, *225*, 1119−1128.
(24) Ramzan, A.; Mehmood, A.; Ashfaq, R.; Andleeb, A.; Butt, H.; Zulfiqar, S.; Nasir, M.; Hasan, A.; Khalid, K.; Yar, M.; Malik, K.; Riazuddin, S. Zinc oxide loaded chitosan-elastin-sodium alginate nanocomposite gel using freeze gelation for enhanced adipose stem cell proliferation and antibacterial properties. *Int. J. Biol. Macromol.* **2023**, *233*, 123519.
(25) Long, Y.; Bai, M.; Liu, X.; Lu, W.; Zhong, C.; Tian, S.; Xu, S.; Ma, Y.; Tian, Y.; Zhang, H.; Zhang, L.; Yang, J. A zwitterionic cellulose-based skin sensor for the real-time monitoring and antibacterial sensing wound dressing. *Carbohydr. Polym.* **2022**, *297*, 119974.
(26) Song, B.; Fan, X.; Gu, H. Chestnut-Tannin-Crosslinked Antibacterial, Antifreezing, Conductive Organohydrogel as a Strain Sensor for Motion Monitoring, Flexible Keyboards, and Velocity Monitoring. *ACS Appl. Mater. Interfaces* **2023**, *15* (1), 2147−2162.
(27) Wang, Y.; Fu, S.; Lucia, L. A.; Zhang, H. A cellulose-based self-healing composite eutectogel with reversibility and recyclability for multi-sensing. *Compos. Sci. Technol.* **2022**, *229*, 109696.
(28) Zhao, L.; Ling, Q.; Fan, X.; Gu, H. Self-Healable, Adhesive, Anti-Drying Freezing-Tolerant, and Transparent Conductive Organohydrogel as Flexible Strain Sensor, Triboelectric Nanogenerator, and Skin Barrier. *ACS Appl. Mater. Interfaces* **2023**, *15* (34), 40975−40990.
(29) Zhan, Y.; Xing, Y.; Ji, Q.; Ma, X.; Xia, Y. Strain-sensitive alginate/polyvinyl alcohol composite hydrogels with Janus hierarchy and conductivity mediated by tannic acid. *Int. J. Biol. Macromol.* **2022**, *212*, 202−210.
(30) Zhang, W.; Xu, L.; Zhao, M.; Ma, Y.; Zheng, T.; Shi, L. Stretchable, self-healing and adhesive sodium alginate-based composite hydrogels as wearable strain sensors for expansion−contraction motion monitoring. *Soft Matter.* **2022**, *18* (8), 1644−1652.
(31) Chen, Y.; Liu, Y.; Li, Y.; Qi, H. Highly Sensitive Flexible Stable, and Hydrophobic Biofoam Based on Wheat Flour for Multifunctional Sensor and Adjustable EMI Shielding Applications. *ACS Appl. Mater. Interfaces* **2021**, *13* (25), 30020−30029.
(32) Gao, Y.-M.; Li, Z.-Y.; Zhang, X.-J.; Zhang, J.; Li, Q.-F.; Zhou, S.-B. One-Pot Synthesis of Bioadhesive Double-Network Hydrogel Patch as Disposable Wound Dressing. *ACS Appl. Mater. Interfaces* **2023**, *15* (9), 11496−11506.
(33) Zeng, L.; Liu, B.; Gao, G. Physically crosslinked polyvinyl alcohol/chitosan-phytic acid hydrogels for wearable sensors with highly conductive, recyclable and antibacterial properties. *Sci. China Mater.* **2023**, *66* (10), 4062−4070.
(34) Liu, Y.; Zhu, M.; Meng, M.; Wang, Q.; Wang, Y.; Lei, Y.; Zhang, Y.; Weng, L.; Chen, X. A dual-responsive hyaluronic acid nanocomposite hydrogel drug delivery system for overcoming multiple drug resistance. *Chin. Chem. Lett.* **2023**, *34* (1), 107583.
(35) Zhang, J.; Wang, Y.; Wei, Q.; Wang, Y.; Li, M.; Li, D.; Zhang, L. A 3D printable, highly stretchable, self-healing hydrogel-based sensor based on polyvinyl alcohol/sodium tetraborate/sodium alginate for human motion monitoring. *Int. J. Biol. Macromol.* **2022**, *219*, 1216−1226.
(36) Wei, H.; Li, A.; Kong, D.; Li, Z.; Cui, D.; Li, T.; Dong, B.; Guo, Z. Polypyrrole/reduced graphene aerogel film for wearable piezoresisitic sensors with high sensing performances. *Adv. Compos. Hybrid Mater.* **2021**, *4* (1), 86−95.
(37) Varaprasad, K.; Raghavendra, G. M.; Jayaramudu, T.; Seo, J. Nano zinc oxide−sodium alginate antibacterial cellulose fibres. *Carbohydr. Polym.* **2016**, *135*, 349−355.
(38) Chen, W.-P.; Hao, D.-Z.; Hao, W.-J.; Guo, X.-L.; Jiang, L. Hydrogel with Ultrafast Self-Healing Property Both in Air and Underwater. *ACS Appl. Mater. Interfaces* **2018**, *10* (1), 1258−1265.
(39) Qiao, H.; Qi, P.; Zhang, X.; Wang, L.; Tan, Y.; Luan, Z.; Xia, Y.; Li, Y.; Sui, K. Multiple Weak H-Bonds Lead to Highly Sensitive, Stretchable, Self-Adhesive, and Self-Healing Ionic Sensors. *ACS Appl. Mater. Interfaces* **2019**, *11* (8), 7755−7763.

https://doi.org/10.1021/acsomega.4c01860
ACS Omega 2024, 9, 16851−16859

(40) Oun, A. A.; Rhim, J.-W. Carrageenan-based hydrogels and films: Effect of ZnO and CuO nanoparticles on the physical, mechanical, and antimicrobial properties. *Food Hydrocolloids* **2017**, *67*, 45−53.
(41) Mohandas, A.; Deepthi, S.; Biswas, R.; Jayakumar, R. Chitosan based metallic nanocomposite scaffolds as antimicrobial wound dressings. *Bioact. Mater.* **2018**, *3* (3), 267−277.
(42) Alavi, M.; Nokhodchi, A. An overview on antimicrobial and wound healing properties of ZnO nanobiofilms, hydrogels, and bionanocomposites based on cellulose, chitosan, and alginate polymers. *Carbohydr. Polym.* **2020**, *227*, 115349.
(43) Zhang, M.; Qiao, X.; Han, W.; Jiang, T.; Liu, F.; Zhao, X. Alginate-chitosan oligosaccharide-ZnO composite hydrogel for accelerating wound healing. *Carbohydr. Polym.* **2021**, *266*, 118100.
(44) Khan, M. I.; Paul, P.; Behera, S. K.; Jena, B.; Tripathy, S. K.; Stålsby Lundborg, C.; Mishra, A. To decipher the antibacterial mechanism and promotion of wound healing activity by hydrogels embedded with biogenic Ag@ZnO core-shell nanocomposites. *Chem. Eng. J.* **2021**, *417*, 128025.
(45) Yao, D.; Wu, L.; Peng, S.; Gao, X.; Lu, C.; Yu, Z.; Wang, X.; Li, C.; He, Y. Use of Surface Penetration Technology to Fabricate Superhydrophobic Multifunctional Strain Sensors with an Ultrawide Sensing Range. *ACS Appl. Mater. Interfaces* **2021**, *13* (9), 11284−11295.
(46) Iwaki, Y. O.; Escalona, M. H.; Briones, J. R.; Pawlicka, A. Sodium Alginate-Based Ionic Conducting Membranes. *Mol. Cryst. Liq. Cryst.* **2012**, *554* (1), 221−231.
(47) Tang, Z.; Bian, S.; Wei, J.; Xiao, H.; Zhang, M.; Liu, K.; Huang, L.; Chen, L.; Ni, Y.; Wu, H. Plant-inspired conductive adhesive organohydrogel with extreme environmental tolerance as a wearable dressing for multifunctional sensors. *Colloids Surf., B* **2022**, *215*, 112509.
(48) Ren, J.; Li, M.; Li, R.; Wang, X.; Li, Y.; Yang, W. Transparent, highly stretchable, adhesive, and sensitive ionic conductive hydrogel strain sensor for human motion monitoring. *Colloids Surf., A* **2022**, *652*, 129795.
(49) Shen, J.; Du, P.; Zhou, B.; Zhang, G.; Tang, X.; Pan, J.; Li, B.; Zhang, J.; Lu, J.; Li, Y. Y. An anti-freezing biomineral hydrogel of high strain sensitivity for artificial skin applications. *Nano Res.* **2022**, *15* (7), 6655−6661.

https://doi.org/10.1021/acsomega.4c01860
ACS Omega 2024, 9, 16851−16859